Electronic structure and the martensitic transformation in β-phase Ni-Al alloys: ^{27}Al NMR and specific-heat measurements

Silvia Rubini and Costas Dimitropoulos
Institut de Physique Expérimentale Ecole Polytechnique Fédérale de Lausanne CH-1015 Lausanne Switzerland

Sergio Aldrovandi and Ferdinando Borsa*
Dipartimento di Fisica "A. Volta," Universita' di Pavia I-27100, Pavia, Italy

David R. Torgeson and Jerzy Ziolo
Ames Laboratory and Department of Physics, Iowa State University Ames, Iowa 50011
(Received 12 May 1992)

^{27}Al NMR line shape, Knight shift, relaxation rates together with low-temperature specific heat and magnetic susceptibiltiy were measured as a function of temperature and external magnetic-field in two Ni-rich β-phase Ni-Al alloys (62% Ni and 63% Ni) undergoing a martensitic phase transformation (MPT) below room temperature. For the purpose of comparison, two further alloys not undergoing the MPT were investigated (50% Ni and 55% Ni). Regarding the electronic properties of the alloys, we find an increase in the density of states at the Fermi level and a decrease of *s*-character of the conduction electron wave function as a function of the increase of Ni content from the 1:1 Ni-Al alloy. Furthermore, the inhomogeneous broadening of the ^{27}Al linewidth indicates that the additional Ni replacing Al at the "wrong" site introduces quasilocalized magnetic states. Regarding the MPT we find a slight decrease of the Knight shift and of the Korringa product $(T_1T)^{-1}$ going from the austenite to the martensite. In the transformation-temperature region, the ^{27}Al NMR line is broadened by the effect of superposition of two signals arising from the austenite and the transforming phase. The deconvolution of the spectrum gives information about the nucleation and growth of the martensite, which appears to be continuous and involving a succession of intermediate states, in contrast with the abrupt nucleation of fully transformed martensite observed in Cu-Zn-Al. No anomalous enhancement of the relaxation rate is observed above M_s or during the MPT. Although the NMR cannot rule out the presence of static precursor effects a few degrees above the transformation temperature M_s, no evidence was found for the formation of martensitic regions well above M_s where tweed patterns are observed by electron microscopy.

I. INTRODUCTION

The martensic phase transformations (MPT's) are displacive phase transformations whose kinetics and morphology are dominated by strain energy.[1] Much attention has been devoted to MPT's in metallic alloys particularly for the shape memory effects associated with the transformation, which lead to important industrial applications.[2] Some of the most interesting systems consist of quenched bcc alloys which undergo on cooling a thermoelastic MPT.[3] From the thermodynamical point of view it is known that the disordered β phase is stabilized at high temperature by vibrational entropy.[4] At low temperature the β phase becomes mechanically unstable with respect to a (110) shear, and it transforms martensically into a more closed-packed structure.[4] In fact, the bcc metastable structure has an inherent lattice instability towards a transverse-acoustic phonon mode propagating along the [110] direction of the cubic lattice.[5,6] The crystal structure in the low-temperature phase (martensite) can be described as a "freezing" of the "soft" phonon accompanied by a macroscopic strain. Although the phonon instability can indicate the path that the MPT will take, it cannot, contrary to the case of quasi-second-order structural transitions, explain alone the MPT and details of the transformation as the nucleation mechanism, the precursor effects, and the role of the conduction electrons.

The Ni-Al alloy forms for the 1:1 stoiochiometry a β phase whose crystal structure is ordered bcc (CsCl type). The β phase has a wide stability range at high temperature, which extends both on the Ni-rich and on the Al-rich side of the composition, but narrow down towards 1:1 with cooling.[7] The Ni-rich β phase, with excess Ni randomly replacing Al, can be retained by rapidly quenching from high temperature to prevent diffusional decomposition. The metastable β phase so obtained will then transform displacively to a more close-packed crystal structure (martensite) at lower temperatures or by application of a stress.[8,9] The structure of the martensite is a monoclinic periodic stacking of three or seven planes ($3M$ or $7M$ structure), depending on the concentration and on the driving force (temperature or strain) of the transformation.[5] The temperature of the beginning of the transformation, M_S, varies very rapidly with composition in the range 60–66 % Ni (Refs. 10 and 11), tracking the step boundary between the stable β phase and the $L1_2$ consisting of an off-stoichiometry $AlNi_3$ phase (see Fig. 1). A recent electronic band calculation in the Ni-Al alloy has shown the importance of electron-phonon in-

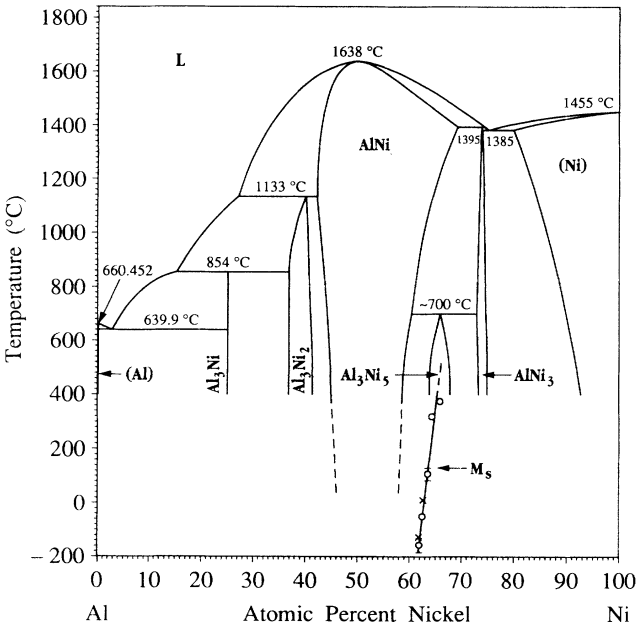

FIG. 1. Assessed Ni-Al phase diagram from Ref. 7. The concentration dependence of the transformation temperature M_S is also reported: circles from Ref. 10 and crosses from the NMR measurements of the present work.

teraction and of the nesting of the Fermi surface in determining the symmetry of the "soft" phonon mode.[12]

Recently, neutron-scattering experiments[13] and theoretical and first-principles calculations[14,15,12] have been applied to try to clarify the microscopic mechanism underlying the transformation. Nuclear magnetic resonance (NMR) and nuclear quadrupole resonance (NQR) techniques provide local microscopic information about structural phase transitions which are complementary to neutron-scattering results. An extensive ^{27}Al and ^{63}Cu NMR study in a bcc CuZn-Al alloy displaying a MPT has established the potential of the technique for the microscopic investigation of this class of transformation.[16] In this paper we present a microscopic investigation by ^{27}Al NMR of the MPT in the β-phase Ni-Al alloys. In order to asses the relevance of the electronic properties on the occurrence of the MPT, we compare the results of two alloys at 63% Ni and 62% Ni, respectively, transforming martensitically to the 7M structure, with the results of two alloys with 50% Ni and 55% Ni, respectively, which do not undergo the MPT but rather fall into the stability range of the β phase. Measurements of the ^{27}Al Knight shift, linewidth and shape, and spin-lattice relaxation rate (T_1^{-1}) will be presented and discussed on terms of changes of the microscopic electronic properties. In order to support the above analysis we have also performed low-temperature specific-heat measurements aimed at determining the density of electronic states at the Fermi level, and magnetic susceptibility measurements vs temperature in the alloys undergoing the MPT. In Sec. II the experimental methods and the procedure of data reduction and analysis are described, followed by the presentation of the experimental results in Secs. III and IV. In Sec. V the experimental results are discussed on terms of the electronic structure of the Ni-Al alloys, and particular attention is paid to the possibility of obtaining useful information about the nucleation and growth process of the martensite from the NMR results. The results of the present analysis are compared with the results obtained by high-resolution electron microscopy (HREM) on Ni-Al alloys.

II. EXPERIMENTAL DETAILS

A. Sample preparation

The alloys investigated were prepared by arc melting in argon atmosphere weighted amounts of high-purity Ni and Al metals. The alloys were homogenized at 1200 °C for 3 days and then rapidly cooled at room temperature. The ingots were crushed in a mortar to obtain small particles suitable for the NMR study which requires a sufficient radio-frequency penetration. Particles of different size were used: large particles with a typical dimension of the order of 1 mm and small particles with a size of the order of 100 μm and less. Measurements were performed both in crushed powders and in powders annealed at 500 °C for 6 h to release stresses. No detectable differences were found in the measurements between annealed and unannealed samples, with the possible exception of the samples of fine powders.

The determination of the transition temperatures by differential scanning calorimetry (DSC) was difficult due to the weakness of the signal, and only for the 63% Ni alloy in large particles could we estimate the beginning and the end of the austenite to martensite transformation by cooling $M_S \simeq 290$ K and $M_F \simeq 260$ K, and for the martensite to austenite transformation by heating $A_S \simeq 270$ K and $A_F \simeq 300$ K, in agreement with the data reported by Au and Wayman.[10] The above transformation temperatures in 63% Ni alloys are consistent with the NMR linewidth and Knight shift data. For the 62% Ni alloy, in which the DSC signal was too weak to allow the determination of M_S and M_F, the values quoted in literature vary from $M_S \simeq 90$ K (Ref. 10) to $M_S \simeq 180$ K (Ref. 11) and even $M_S \simeq 275$ K (Ref. 11) depending on sample preparation and thermal treatment. The NMR data in our 62% Ni alloy are consistent with M_S in the neighborhood of 150 K.

The 63% Ni and 62% Ni β-phase Ni-Al alloy samples, which undergo the MPT, were cycled 20 times across the transformation before performing the NMR measurements in order to stabilize the transformation temperatures.

B. Specific heat and magnetic susceptibility

The specific-heat measurements were performed with a standard heat-pulse adiabatic calorimeter between 4 and 40 K and using calibrated germanium resistors as temperature sensors. The sample was first cooled by thermal contact with a liquid-helium bath and the measurements were performed on heating. The resolution of the measurements is typically of the order of 0.01 K. The heat

capacity of the addenda is of the order of 20–50 % of the total heat capacity, depending on the temperature interval. The uncertainty in the specific-heat measurements is estimated to be of the order of 2–3 %.

The magnetic susceptibility measurements were carried out by Paleari (University of Milan) on a Faraday magnetic balance in fields up to 11 kG on powdered samples of about 300 mg. The sensitivity of the instrument, for constant field measurements, is limited by the minimum detectable force (about 10^{-8} N) resulting in a minimum detectable susceptibility of about 10^{-9} cm^3/g. The accuracy of the data is estimated within about 10% of the final value. All samples were measured from 100 K up to room temperature by using a variable temperature cryogenic apparatus with a controlled temperature stabilization of about 0.1 K.

C. NMR measurements

The NMR measurements were performed mainly with a modified Bruker SXP pulse spectrometer in quadrature detection and an Oxford superconducting magnet operating at 7 T. The Knight shift measurements are referred to the ^{27}Al resonance frequency in an $AlCl_3$ aqueous solution. The temperature was stabilized to better than 0.2 K using an Oxford flow cryostat, and monitored continuously by means of a thermocouple imbedded in the sample. All measurements were performed at constant equilibrium temperaure during the cooling of the sample in order to avoid hysteresis effects. Special care was necessary to avoid radio-frequency heating of the sample during the measurements.

The ^{27}Al absorption spectra, obtained by a Fourier transform of the free induction decay (FID) contains a broad background (~50 kHz wide) symmetrically superimposed on the main signal (~5–9 kHz wide). From measurements as a function of the radio-frequency pulse length and as a function of the external magnetic field we could establish that the broad line is due to a distribution of satellite transitions, arising from a fraction of the ^{27}Al nuclei experiencing a nonuniform distribution of first-order quadrupole effects. The linewidth data reported in Sec. IV were obtained by fitting the main line with a Gaussian shape function whose width Δ corresponds to the square root of the second moment of the line, after having subtracted off the broad background component.

The spin-lattice relaxation rate T_1^{-1} was measured by monitoring the regrowth of the FID signal after a saturating sequence of 30 pulses, and was found to be exponential. Since the quadrupole effects are weak, all lines can be completely saturated and the experimental recovery of the magnetization yields $T_1^{-1}=2W_M$,[17] where W_M is the magnetic relaxation transition probability.

III. RESULTS

A. Specific heat

The constant pressure specific heat was measured in the temperature interval 5–20 K to determine the coefficient γ of the linear term which is a measure of the density of electronic states at the Fermi level.[18] In the temperature range 5–11 K, the data can be fitted by the expression[18]

$$C_p=\gamma T+\frac{234R}{\theta_D^3}T^2 , \tag{1}$$

where R is the perfect gas constant. The fit of the experimental data for the two alloys undergoing the MPT is shown in Fig. 2. The values obtained for the parameter γ and for the Debye temperature θ_D are summarized in Table I for the four alloys investigated, together with values from the literature pertaining to the pure metals. The value of the density of states at the Fermi level can be estimated from the specific heat, i.e., $D(E_F)=3\gamma/\pi^2k_B^2$ by neglecting electron-phonon enhancement effects.

B. Magnetic susceptibility

The experimental room-temperature susceptibility χ_{exp} is summarized in Table II for the different alloys. In the temperature range 100–300 K the change of χ_{exp} is less than 10%, and no measurable variation can be ascribed to the presence of the MPT. The lack of effects on χ in β Ni-Al can be contrasted with that observed on Ni-Ti alloys at the MPT, where a decrease of χ by about 30% is observed at the MPT.[19]

A number of parameters, which can be useful in the discussion of the NMR results, is estimated on the basis of the specific heat and the susceptibility measurements (see Table II).

The spin susceptibility χ_{scp} is obtained from the formula[21]

$$\chi_{scp}=\frac{3\mu_B^2}{\pi^2k_B^2}\gamma \tag{2}$$

and the values of γ in Table I (μ_B=Bohr magneton). The spin susceptibility is given by the experimental data after correcting for the ionic and conduction electron diamagnetism:[22]

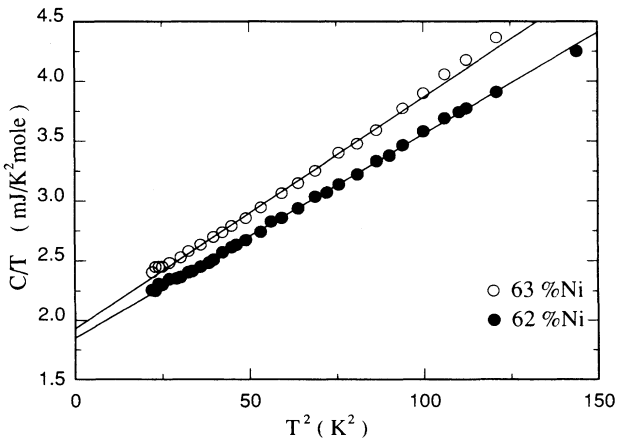

FIG. 2. Results of the low-temperature specific-heat measurements for the 63% Ni and the 62% Ni alloys.

TABLE I. Parameters estimated from the fit of the low-temperature specific-heat measurements with Eq. (1) in the text.

Alloy composition	γ (mJ/K^2 mol)	θ_D (K)	$D(E_F)$ (states/Ry cell)
Ni metal	7.02[a]	375[b]	
Al metal	1.35[a]	394[b]	
0.5 Ni-0.5 Al	0.93±0.05	570	10.8
0.55 Ni-0.45 Al	1.22±0.05	465	14.1
0.62 Ni-0.38 Al	1.85±0.03	485	21.4
0.63 Ni-0.37 Al	1.93±0.03	465	22.3

[a]Reference 21.
[b]Reference 18.

$$\chi_S = \frac{\chi_{\text{exp}} - \chi_{\text{ion}}}{1 - 1/3(m/m^*)^2} , \tag{3}$$

where the effective mass (m/m^*) is given by the ratio of the calculated free-electron density of states at the Fermi level $D(E_F) = m/(\pi\hbar)^2(3\pi^2 n)^{1/3} V_c = 4.64 Z^{1/3}$ (states/Ry cell) (Ref. 18) (where Z is the number of conduction electrons per unit cell and V_c is the cell volume) and the one obtained from the specific-heat measurements (see Tables I and II). In calculating the free-electron density n, three Al valence electrons and one Ni valence electron were taken into account. This is suggested by band-structure calculations which indicate a d^9 corelike configuration for the Ni atom in the alloy.[12] The bcc unit cell of the β-phase alloys has a lattice parameter $a = 2.81$ Å. The comparison of the spin susceptibility estimated from the specific-heat density of states χ_{scp} [Eq. (2)] and the value χ_S deduced from the experiments [Eq. (3)] allows one to drive the Stoner exchange enhancement factor α defined by [21]

$$\chi_S = \frac{\chi_{\text{scp}}}{1 - \alpha} . \tag{4}$$

The value of α obtained from the data in Table II is close to $\alpha = 0.44 \pm 0.02$ for all β-phase alloys, compared with $\alpha = 0.18$ for the Al metal.

IV. ^{27}Al NMR RESULTS

A. Linewidth

The ^{27}Al linewidth Δ, as defined in Sec. II C, was measured both as a function of the temperature and as a function of the external magnetic field. The magnetic field dependence is roughly linear with a zero-field extrapolated values of the order of 2–3 kHz which is close to the root-mean-square second moment calculated from the Van Vleck formula for the nuclear-dipolar interaction of ^{27}Al (the Ni nuclear moments give a negligible contribution). The field dependence of the ^{27}Al linewidth at room temperature is given in Table III for the different alloys investigated. The temperature dependence of the ^{27}Al linewidth is shown in Fig. 3 for the two alloys undergoing the MPT. Here one should distinguish two effects: an almost liner background temperature dependence, associated with the electronic properties of the alloys, and an anomalous broadening in the region of the thermoelastic transformation. The increase in the linewidth in the tempeature region of the martensitic transformation is indicative of the coexistence of two signals slightly shifted; one with respect to the other and originating from the austenite and the martensite as will be discussed in the next section. Linewidth measurements in the other two

TABLE II. Summary of the experimental values of the room-temperature susceptibility, together with the values of the spin susceptibility estimated from the specific heat and from the susceptibility measurements as explained in the text.

Alloy composition	$10^6\chi_{\text{exp}}$ (emu/mol)	$10^6\chi_{\text{dia}}^{\text{ion}}$ (emu/mol)	$10^6\chi_{\text{scp}}$ (emu/mol)	$10^6\chi_S$ (emu/mol)	$\frac{m^*}{m}$
Ni metal		−13[a]			
Al metal	16.3[b]	−2.8[b]	18.5	22.6	1.47
0.5 Ni-0.5 Al	12.0[a]	−7.9[c]	12.7	22.8	1.6
0.55 Ni-0.45 Al	18.5[d]	−8.4[c]	16.7	28.8	2.24
0.62 Ni-0.38 Al	34.5	−9.1[c]	25.3	45.0	3.63
0.63 Ni-0.37 Al	36.4	−9.2[c]	26.7	46.6	3.84

[a]Reference 20.
[b]Reference 21.
[c]This value has been calculated as a weighted average of $\chi_{\text{dia}}^{\text{ion}}$ pertaining to the Al and Ni ions in the corresponding pure metals.
[d]Reference 28.

TABLE III. Summary of the NMR experimental parameters.

Alloy composition	K (%) (Room temp.)	$(T_1T)^{-1}$ $(s^{-1}K^{-1})$	$\frac{d(\delta H)}{dH}$ (Room temp.)
Al metal	0.160[a]	54×10^{-2}[a]	0
0.5 Ni-0.5 Al	0.060	3.24×10^{-2}	$\sim10^{-5}$
0.55 Ni-0.45 Al	0.0676	3.71×10^{-2}	$\sim10^{-4}$
0.62 Ni-0.38 Al	(*A*) 0.069	4.0×10^{-2}	$\sim10^{-4}$
	(*M*) 0.602	3.2×10^{-2}	
0.63 Ni-0.37 Al	(*A*) 0.0685	4.0×10^{-2}	$\sim10^{-4}$
	(*M*) 0.0602	3.2×10^{-2}	

[a]Reference 21

alloys show a similar temperature dependence but without the maximum due to the MPT.

B. Knight shift

The Knight shift vs T decreases smoothly as one goes through the MPT for both samples with 63% Ni and 62% Ni. Since the linewidth (see Fig. 3) goes through a maximum in the transformation temperature interval, one should infer that in the region of the thermoelastic transition two signals coexist, one from the martensite and the other from the austenite, as will be discussed in the next session. Thus the measured Knight shift shown in Fig. 4 represents the values of K in the high-temperature austenitic phase and in the low-temperature martensitic phase, while in the transformation region the value of K represents a weighted average for the two phases. It is noted that by comparing the Knight shift for particles of different size one can infer that in the small-particle samples a fraction of austenite remains untransformed even at low temperature. The results for the temperature-independent Knight shift in the β-phase alloys which do not undergo the MPT are given in Table III. These values are in good agreement with previous measurements in Ni-Al alloys as a function of composition at fixed temperature and fixed external magnetic field.[23]

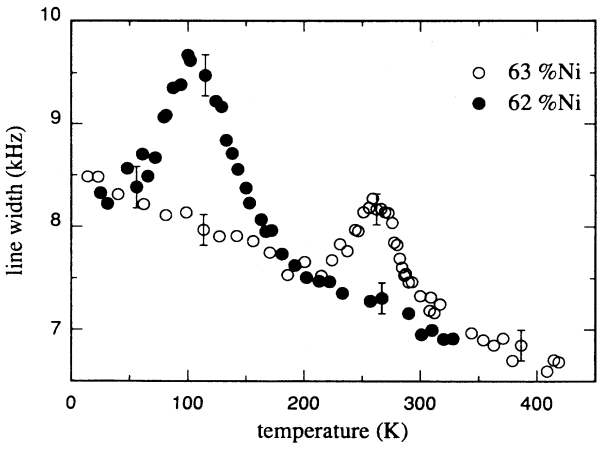

FIG. 3. ^{27}Al linewidth (central line) as a function of temperature for the 63% Ni and 62% Ni alloys in large particles. The width, as obtained from the Gaussian best fit of the experimental absorption spectra, corresponds to the square root of the second moment.

C. Nuclear spin-lattice relaxation rate

The ^{27}Al nuclear spin-lattice relaxation rate T_1^{-1} vs temperature is shown in Fig. 5 for the large-particle 62%

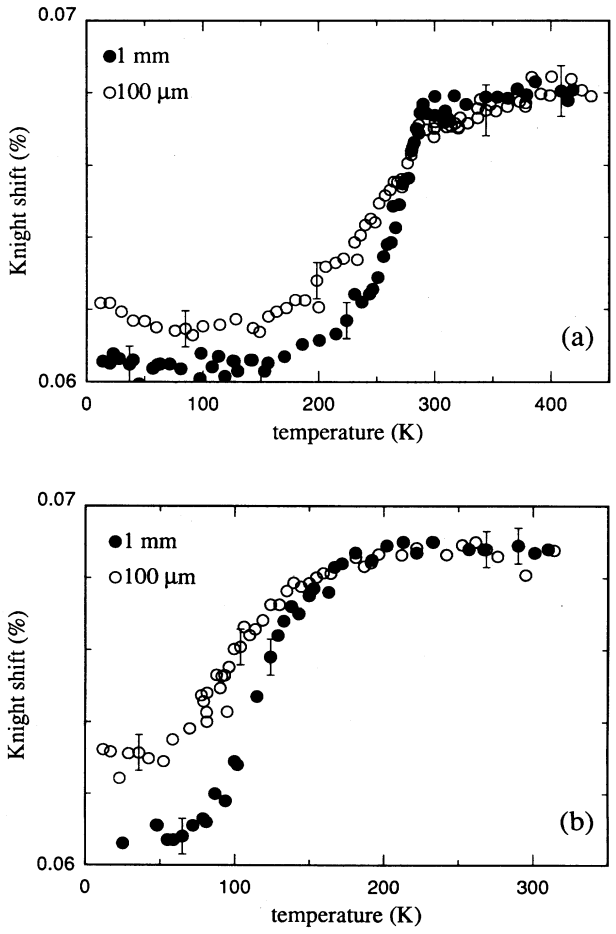

FIG. 4. ^{27}Al Knight shift as a function of temperature (a) 63% Ni, (b) 63% Ni. In both cases the results obtained on the large-particle and on the small-particle samples are reported.

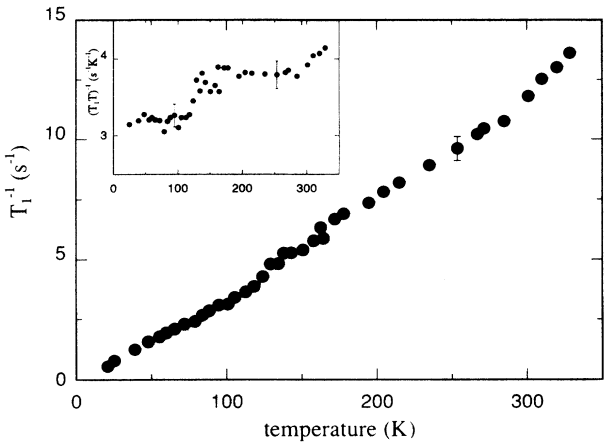

FIG. 5. ^{27}Al spin-lattice relaxation rate T_1^{-1} as a function of temperature for the 62% Ni alloy. In the inset is reported the corresponding Korringa ratio $(T_1T)^{-1}$ vs temperature (in K).

Ni sample. Above and below the MPT, T_1^{-1} follows a Korringa-type linear temperature dependence with a change of slope which is consistent with the change of Knight shift between the austenite and the martensite (see Fig. 4). No anomalous enhancement of T_1^{-1} is obsevable in the transition temperature region, contrary to what was found for both ^{27}Al and ^{63}Cu in Cu-Zn-Al alloys.[16] The two alloys without the MPT also display a T_1^{-1} which depends linearly on temperature. The values for the product $(T_1T)^{-1}$ are summarized in Table III for the different alloys.

V. DISCUSSION

A. Electronic structure and MPT

1. *Knight shift and spin-lattice relaxation rate*

The density of states (DOS) at the Fermi level as derived from the γ values in Table I increases by a factor of 2 as the Ni concentration increases from the 1:1 ratio towards the stability limit of the β phase in the Ni-Al alloy. The increase should be attribted to the Ni d band crossing the Fermi level as indicated by the increase in the estimated effective mass m^* (see Table II). Correspondingly, the Knight shift varies only slightly (see Table III) indicating that core polarization effects and orbital contributions, which are related to d-electrons, have negligible effects on the ^{27}Al Knight shift. Assuming a dominant s contribution one can write, for the Knight shift,

$$K=\frac{1}{\mu_B}\frac{\chi_S}{N_A}H_{\text{eff}}\xi\ , \tag{5}$$

and by assuming for the atomic hyperfine field $H_{\text{eff}}=190$ T (Ref. 21) and the spin susceptibility χ_S reported in Table II, one can estimate the following fractions of s character of the conduction electron wave functions at the Fermi level: 50% Ni ($\xi=0.08$); 55% Ni ($\xi=0.07$); 62% Ni ($\xi=0.045$); 63% Ni ($\xi=0.043$). The small value of ξ, when compared to $\xi=0.2$ in pure Al metal, indicates a prevalent d character of the DOS at the Fermi surface, becoming more pronounced with increasing Ni concentration. This is entirely consistent with recent band-structure calculations[12] which found a total d-band occupation close to nine electrons per Ni atom and a sharp peak in the DOS just below E_F in equiatomic Ni-Al. Within this scheme, the addition of Ni produces a lowering of the total conduction electron density, with a consequent lowering of E_F towards the sharp peak which may broaden somewhat as a result of disorder.

Regarding the MPT in the two Ni-rich alloys, one notes that the overall change of the Knight shift between the austenitic and the martensitic phase is about 10%, the same as found in Cu-Zn-Al alloys[16] (see Fig. 4). On the other hand, the magnetic susceptibility changes very little in the temperature interval 100–300 K, which includes the transformation in the case of the 63% Ni alloy, indicating a negligible change in the total DOS at the Fermi level occurring at the MPT. Since, as we have seen above, the Knight shift is not very sensitive to changes in the total DOS, the decrease of K should be entirely ascribed to a decrease of ξ, the fraction of the s character of the conduction electron wave function at the Fermi surface.

The nuclear spin-lattice relaxation rate follows a Korringa-type linear temprature dependence:[21]

$$T_1^{-1}=\frac{4\pi k_B}{\hbar}\left[\frac{\gamma_N}{\gamma_e}\right]^2 k(\alpha)K^2T\ , \tag{6}$$

where γN and γ_e are the gyromagnetic ratios of the nucleus and of the electron, and $k(\alpha)$ is en enhancement factor associated with the exchange and correlation effects in the conduction electron Fermi gas and α is the Stoner exchange factor [see Eq. (4)]. From the experimental values of $(T_1T)^{-1}$ and K in Table III and Eq. (6), one can estimate $k(\alpha)=0.32\pm0.03$, the same for all β-phase alloys both in the austenitic and in the martensitic phases. The enhancement α of the uniform susceptibility estimated in Sec. III, namely, $\alpha=0.44\pm0.02$, is also practically constant in all β-phase alloys. The relation between $k(\alpha)$ and α departs from the Warren-Shaw result,[24] i.e., $K(\alpha)\simeq 1-\alpha$, which is obeyed in simple free-electron-like metals with a spherical Fermi surface. This is consistent with exchange and correlation effects which are strongly wave-vector dependent as expected for a marked anisotropy of the Fermi surface. The small change in both Knight shift and susceptibility at the MPT together with the constant values for $k(\alpha)$ and α are taken as indications that the MPT is not related to important changes of the electronic band structure of the alloy.

2. *^{27}Al NMR linewidth*

The magnetic field-dependent part of the ^{27}Al linewidth can be explained by the presence of a distribution of Knight shift values at the Al nuclear site which is of the order of 2% of the average value for the 50% Al alloy and about 20% for the other β-phase alloys (see Table III). The anomalous broadening of the line ob-

served in the transformation temperature range is not considered here and will be discussed in Sec. V B. Since the percentage of paramagnetic impurities present in our samples can be estimated to be less than 0.01% and since the observed magnetic broadening appears to increase significantly in the disordered Ni-rich alloys, one can safely conclude that the inhomogenous broadening is an intrinsic effect. The randomness in the location of the excess Ni, which replaces Al in the otherwise ordered bcc structure, produces a distribution of local environment at a given Al nuclear site, due to the second-nearest-neighbor probability distribution of Ni and Al atoms. If the magnetic broadening were to arise from the charge-density oscillations around the Ni atoms on the "wrong sites," the broadening would be temperature independent, contrary to the experimental findings (see Fig. 3). Thus we propose, on the basis of the NMR linewidth data, that Ni atoms which replace the Al in the Ni-Rich β-phase alloys introduce quasilocalized d states, whereby the spin-density oscillations around these virtual bound d states[25] should account for the observed temperature-dependent inhomogeneous broadening. It is likely that the virtual bound d states are related to the sharp peak in the DOS just below E_F found in the band-structure calculations.[12] The inhomogeneous broadening is proportional to the local spin susceptibility of the quasi-localized moments which we assume to be described by a Curie-Weiss term. The experimental ^{27}Al NMR linewidth Δ can then be fitted by

$$\Delta(H,T)=\Delta(0,\infty)+\frac{C}{T+\theta}H \ , \tag{7}$$

where $\Delta(0,\infty)=1.99$ kHz corresponds to the calculated Van Vleck dipolar broadening[26] and the second term in Eq. (7) is due to the random distribution of Ni atoms in the "wrong" sites, which are second-nearest neighbors to a given Al nucleus. From the fit of the data in the two alloys undergoing the MPT (see Fig. 3) one finds $\theta=1010$ K and $C=96.5$ Hz K G^{-1}. The large effective Curie-Weiss temperature θ is typical of strongly exchange enhanced itinerant antiferromagnets.[27] A confirmation for the presence of almost localized moments can be found in the magnetic susceptibility. In fact, a considerable increase in the temperature dependence of χ was indeed observed upon increasing the Ni concentration of the Ni-Al β-phase alloys and it was attributed to the appearance of $3d$ holes.[28] In our alloys the measurements performed in the temperature range 100–300 K do not allow an unambiguous separation of the contributon to the temperature dependence of χ due to quasi-local moments from the one due to the MPT since both effects are too small.

B. Nucleation and growth of the martensite and precursor effects

From Fig. 4 one can see that the Knight shift of the high-temperature austenitic phase exceeds the one of the martensitic phase by about 10%, correspondng to a shift of the line of 7 kHz at 7 T. Thus, the broadening of the ^{27}Al line observed in the transformation temperature range is interpeted as the superposition of signals with different shifts arising from regions of the sample in different phases. Over the whole transformation temperature range the ^{27}Al line remains symmetric, whereby the broadening and the progressive shift of the center of gravity of the line denote the occurrance of the transformation. This represents an important difference from the Cu-Zn-Al case were an asymmetry of the ^{27}Al line was clearly observed,[16] and from the Ag-Cd case, where two resolved lines are present between M_S and M_F.[29]

An analysis of the spectra as a function of temperature can give information about the transformation temperatures and the process of nucleation and growth of the martensite, similar to the case of Cu-Zn-Al.[16] Although the analysis is difficult due to the lack of resolution (the 7-kHz shift is just comparble to the half-width of the NMR line), some unambiguous semiquantitative results can be nevertheless obtained as described below. In the temperature region of the transformation, the NMR line was fitted by the superposition of two Gaussians. If the two lines are assumed to be centered at the resonance frequencies of the austenite and the martensite, as expected for the coexistence of the two well-identified phases, the fit is poor. In order to have a good fit we had to assume that while the austenite line remains fixed at the austenite frequency, the second one, arising from the part of the sample which is transforming, is centered at a frequency which is a function of temperature. To reduce the number of parameters in the fit, we assume the center of the second line to shift proportionally with the fraction of the transforming phase already present. Furthermore, the linewidth of the austenite line has been calculated at each temperature according to the observed background behavior, while that of the second line has been left as a free parameter in the fit.

The results so obtained for the linewidth and the Knight shift of the transformed phase as a function of temperature are shown in Figs. 6 and 7 for the two alloys 63% Ni and 62% Ni, respectively, together with the raw experimental data already reported in Figs. 3 and 4; while in Fig. 8 is reported the fraction of martensite vs T for both alloys.

From the results of the fit, two main features become apparent which we believe do not depdend critically on the parametrization used in the fit. The first feature is the gradual rather than abrupt variation of the Knight shift of the transforming phase which is a function of the amount of the transforming phase present in the temperature region where both phases coexist. The second feature, which is related to the first one, consists of the broadening of the line arising from the transforming phase, again only in the transformation temperature range. The picture emerging from the above results is one of a continuous formation of nuclei of martensite with an incomplete degree of deformation. The growth of each nucleus is accompanied by a progressive lattice deformation, up to the fully transformed martensite structure. At each temperature, regions of the sample at a different degree of deformation between the austenitic and the martensitic structure coexist in thermoelastic equilibrium, as indicated by the distribution of the

Knight shift which generates the broadening of the NMR line of the transforming phase.

No experimental method seems to be able to follow as a function of temperature and with sufficient precision the lattice parameters of the transforming phase during the thermoelastic transformation. However, indirect confirmations of the pictures of a continuous transformation with a gradual increase in the distortion of the lattice from the austenite up to the fully transformed martensite can be found in results obtaned by high-resolution electron microscopy (HREM) in Ni-Al alloys[30,31] at a fixed temperature. The first result concerns stress-induced martensite around a nanocrack in a 63% Ni alloy.[30] The structure of the stress-induced martensite at this composotion is $3M$. This structure is indeed observed near the crack, where the stress is higher, but the distortion of the structure decreaes with increasing distance from the crack. Between the $3M$ region and the austenite region, a long-period stacking structure, similar to the $7M$ structure, with a decreasing degree of deformation is also observed. Similar results have been obtained at room temperature on a Ni-Al sample with an M_S slightly above room temperature.[31] Again the equilibrium martensite

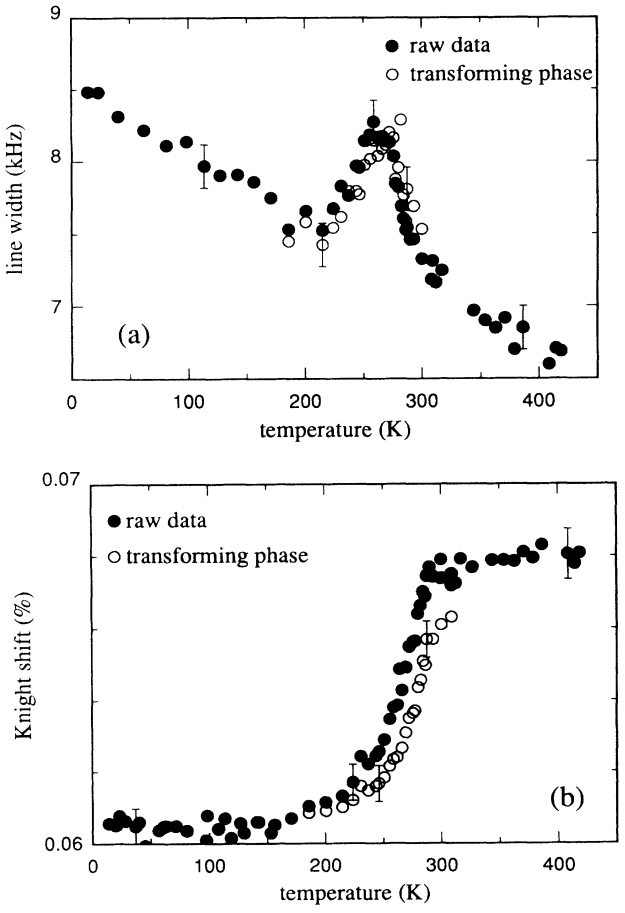

FIG. 6. (a) Linewidth Δ and (b) Knight shift of the transforming phase, as obtained by the deconvolution of the spectra for the 63% Ni alloy in large particles. The raw data are reported for the sake of comparison.

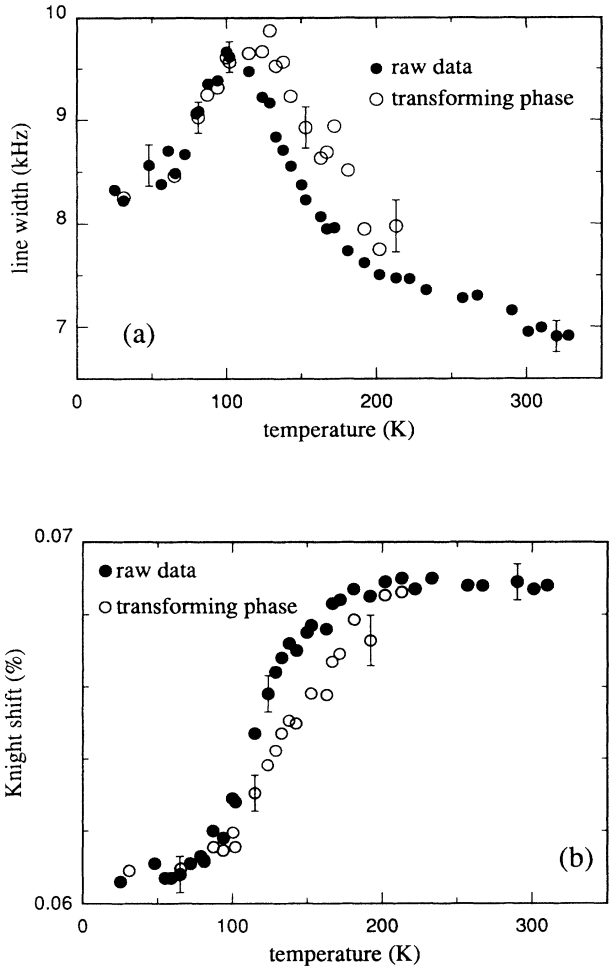

FIG. 7. (a) Linewidth Δ and (b) Knight shift of the transforming phase vs temperature, as obtained by the deconvolution of the spectra, for the 62% Ni alloy in large particles. The raw data are reported for sake of comparison.

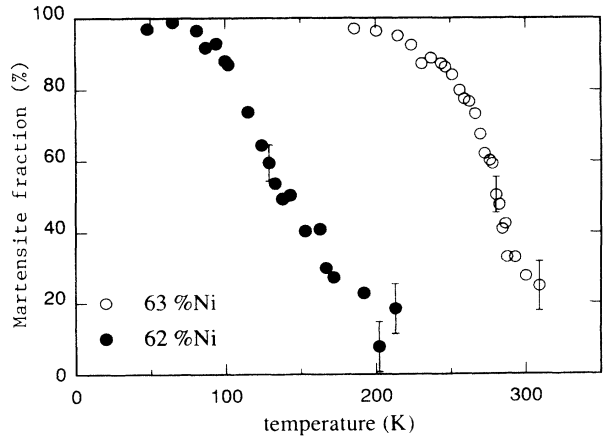

FIG. 8. Fraction of the transforming phase present in the sample as a function of temperature for the 63% Ni and 62% Ni alloys in large particles.

structure is $3M$. No sharp interfaces between austenite and martensite have been observed. The amount of deformation gradually decreases toward the side of the martensite plate, and on the edege of the plate some intermediate distortions are found.

VI. CONCLUSIONS

From the analysis of the ^{27}Al NMR results in conjunction with those of the low-temperature specific heat and the magnetic susceptibility, we find that the ordered β-phase Ni-Al alloy with 1:1 composition is characterized by an almost filled d band with a relatively low DOS at the Fermi level, and a large mixing among d states of Ni and sp states of Al at the Fermi level. In the Ni-rich β-phase alloys, the total DOS at the Fermi level increases, indicating a shift of E_F towards a peak in the d-band DOS just below the Fermi level, in good agreement with the recent electronic band-structure calculations.[12] We also find evidence for the formation of quasilocalized d states associated with Ni atoms replacing the Al atoms on the "wrong" site, whereby the local spin susceptibility of these quasilocalized magnetic moments is responsible for the inhomogeneous broadening of the ^{27}Al NMR line. The MPT occurring in the 63% Ni and the 62% Ni alloys is not accompanied by relevant changes of the electronic band structure, but only by minor rearrangements of the nearest-neighbor and second-nearest-neighbor bonding orbitals with a consequent decrease of s character of the wave function at the Fermi level. The nucleation and growth of the martensitic phase is rather continuous compared with Cu-Zn-Al alloys. The Knight shift of the transforming phase appears to change smoothly during the temperature interval of the thermoelastic transformation. This result suggests that the MPT in Ni-Al alloys takes place via a sequence of successive distortions of the lattice from the original bcc structure up to the final $7M$ phase. This situation is to be contrasted with Cu-Zn-Al alloys where it was found that the nucleation of the martensite is explosive and the martensitic structure forms with its final lattice deformation already built in. The broadening and shifting of the NMR line start close to M_S as measured by DSC. Howeer, since the temperature M_S at which the MPT initiates is ill defined both in the NMR results and in DSC, it is difficult to decide whether the initial broadening of the NMR line is due to the formation of martensite or to precursor effects in the form of static distortions of the lattice. It should be noted that static precursor effects can be detected by NMR only if the wavelength of the modulation of the strain field is comparable to the unit cell. Regarding dynamic effects, no anomaly was detectable in the nuclear spin-lattice relaxation rate, neither above M_S or in the transformation temperature range between M_S and M_F. This negative result can be taken as an indication that local precursor embryonic fluctuations, if present, are very fast ($\tau \leq 10^{-12}s$). Furthermore the charge-density fluctuations occurring at the interfaces between austenite and transforming phase during the growth of the martensite must be much smaller than, for example, in Cu-Zn-Al, where an anomalous increase of T_1^{-1} in the region $M_S - M_F$ was observed. It is noted tht the apparent lack of critical effects on approaching the MPT reported here is in favor of the idea that these transformations belong to the class of the nucleation transitions rather than instability transitions. An example of the nucleation transition is the formation of vortex lines at the critical field H_{C-1} in type-II superconductors. In this case it was argued by de Gennes[32] that instead of defining an order parameter in the Landau sense one could define a pseudoorder parameter in terms of topological constraints such as the number of vortex lines entering the sample at H_{C-1}. By analogy, one could define an order parameter at the MPT in terms of the percentage of martensitic phase nucleating in the sample at M_S. It has been documented here that an order parameter so defined can be measured by NMR and that in terms of such an order parameter the MPT in different alloys can be discontinuous (Cu-Zn-Al) or continuous (Ni-Al).

ACKNOWLEDGMENTS

This work was supported in part by the Swiss National Foundation for Scientific Research. Ames Laboratory is operated for the U.S. Department of Energy by Iowa State University under Contract No. W-7405-ENG-82. The work at the Ames Laboratory was supported by the Office of Basic Energy Sciences. The work at Pavia University was supported by INFM-GNSM (grant MPI 40%). Thanks are due to Dr. A. Paleari for performing the magnetic susceptibility measurements and to Professor B. H. Harmon for useful discussions.

*Also Ames Laboratory and Department of Physics, Iowa State University, Ames, Iowa 50011.

[1]Z. Nishiyama, *Martensitic Transformations* (Academic, New York, 1978).

[2]See various contributions in, *The Martensitic Transformation in Science and Technology,* edited by E. Hornbogen and N. Jost (DMG Informationgesellschaft Verlag, Overnosel, Germany, 1989).

[3]L. Delay, R. V. Krishnan, H. T. Tas, and H. Warlimont, J. Mater. Sci. **9**, 1521 (1974); R. V. Krishnan, K. Delaey, H. T. Tas, and H. Warlimont, *ibid.* **9**, 1536 (1974); H. Warlimont, L. Delaey, R. V. Krishnan, and H. Tas, *ibid.* **9**, 1545 (1974).

[4]C. Zener, in *Phase Stability in Metals and Alloys,* edited by P. S. Rudman, J. Stringer, and R. I. Jaffee (McGraw-Hill, New York, 1967).

[5]G. Guenin, D. Rios Jara, M. Morin, L. Delaey, R. Pynn, and P. F. Gobin, J. Phys. (Paris) Colloq. **43**, C4-597 (1982).

[6]S. M. Shapiro, B. X. Yang, G. Shirane, Y. Noda, and L. E. Tanner, Phys. Rev. Lett. **62**, 1298 (1989).

[7]M. F. Singleton, J. L. Murray, and P. Nash, in *Binary Alloy Phase Diagrams,* edited by T. B. Massalski (American Society for Metals, Metals Park, OH, 1986).

[8]V. V. Martynov, K. Enami, L. G. Khandros, A. V. Tkachenko, and S. Nenno, Scr. Metall. **17**, 1667 (1983).

[9]Y. Noda, S. M. Shapiro, G. Shirane, Y. Yamada, and L. E. Tanner, Phys. Rev. B **42**, 10 397 (1990).
[10]Y. K. Au and C. M. Wayman, Scr. Metall. **6**, 1209 (1972).
[11]S. Ochiai and M. Ueno, J. Jpn. Inst. Met. **52**, 157 (1988).
[12]G. L. Zhao and B. N. Harmon, Phys. Rev. B **45**, 2818 (1992).
[13]L. E. Tanner, D. Schryvers, and S. M. Shapiro, Mater. Sci. Eng. A **127**, 2051 (1990).
[14]Y. Chen, K. M. Ho, and B. N. Harmon, Phys. Rev. B **37**, 283 (1988).
[15]R. J. Gooding and J. A. Krumhansl, Phys. Rev. B **39**, 1535 (1989).
[16]S. Rubini, C. Dimitropoulos, R. Gotthardt, and F. Borsa, Phys. Rev. B **44**, 2019 (1991).
[17]A. Avogadro and A. Rigamonti, in *Proceedings of the XXII Congress Ampere,* edited by V. Hovi (North-Holland, Amsterdam, 1973), p. 255.
[18]N. W. Ashcroft and N. D. Mermin, *Solid State Physics* (Holt-Saunders, New York, 1976).
[19]A. Paleari (unpublished).
[20]J. A. Seitchik and R. H. Walmsley, Phys. Rev. **131**, 1473 (1963).
[21]G. C. Carter, L. H. Bennet, and D. J. Kahan, *Metallic Shifts in NMR* (Pergamon, New York 1977).
[22]A. H. Wilson, *The Theory of Metals* (Cambridge University Press, Cambridge, 1965).
[23]J. Crousier, J. P. Crousier, and R. Streiff, Acta Metall. **25**, 619 (1977).
[24]R. W. Shaw and W. W. Warren, Phys. Rev. B **3**, 1562 (1971).
[25]J. Friedel, Nuovo Cimento Suppl. **7**, 287 (1958).
[26]A. A. Abragam, *The Principles of Nuclear Magnetism* (Clarendon, Oxford, 1961).
[27]T. Moriya, *Spin Fluctuations in Itinerent Electron Magnetism* (Springer-Verlag, Berlin, 1985).
[28]K. Miyatani and S. Iida, J. Phys. Soc. Jpn. **25**, 1008 (1968).
[29] ^{113}Cd NMR measurements are presently underway on a Ag 46.5% Cd alloy displaying a MPT at $M_S = 143$ K. The detailed results will be published elsewhere.
[30]D. Schryvers and L. E. Tanner, Micron and Microsc. Acta **20**, 153 (1989).
[31]D. Schryvers, Habilitation Arbeit Vrije Universiteit Bruxell (B), 1991.
[32]P. G. de Gennes, in *Fluctuations, Instabilities, and Phase Transitions,* edited by T. Riste (Plenum, New York, 1973).